Kurdistan Journal of Applied Research (KJAR)
Print-ISSN: 2411-7684 | Electronic-ISSN: 2411-7706

Original paper

Check for updates

A Wavelet Shrinkage Mixed with a Single-level 2D Discrete Wavelet Transform for Image Denoising

Hawkar Qasim Birdawod [a], **Azhin Mohammed Khudhur** [b], **Dler Hussein Kadir** [b*], **Dlshad Mahmood Saleh** [b,c]

[a] Department of Business Administration, College of Administration and Financial Sciences, Cihan University-Erbil, Erbil, Iraq
[b] Department of Statistics and Informatics, College of Administration and Economics, Salahaddin University, Erbil, Iraq
[c] Department of Accounting and Financial, College of Administration and Economics, Lebanese French University, Erbil, Iraq

Submitted: 5 March 2024
Revised: 17 May 2024
Accepted: 27 June 2024

* Corresponding Author:
dler.kadir@su.edu.krd

Keywords: Denoising image, Single-level 2D DWT, Wavelet, Bayesshrink threshold, Daubechies (db7), Coiflets (coif5), Fejér-Korovkin (fk4).

How to cite this paper: H. Q. Birdawod, A. M. Khudhur, D. H. Kadir, D. M. Saleh, "A Wavelet Shrinkage Mixed with a Single-level 2D Discrete Wavelet Transform for Image Denoising", KJAR, vol. 9, no. 2, Jun. 2024, doi: 10.24017/science.2024.2.1

Abstract: The single-level 2D discrete wavelet transform method is a powerful technique for effectively removing Gaussian noise from natural images. Its effectiveness is attributed to its ability to capture a signal's energy at low energy conversion values, allowing for efficient noise reduction while preserving essential image details. The wavelet noise reduction method mitigates the noise present in the waveform coefficients produced by the discrete wavelet transform. In this study, three different wavelet families—Daubechies (db7), Coiflets (coif5), and Fejér-Korovkin (fk4)—were evaluated for their noise removal capabilities using the Bayes shrink method. This approach was applied to a set of images, and the performance was analyzed using the Mean Squared Error (MSE) and Peak Signal-to-Noise Ratio (PSNR) metrics. Our results demonstrated that among the wavelet families tested, the Fejér-Korovkin (fk4) wavelet consistently outperformed the others. The fk4 wavelet family yielded the lowest MSE values, indicating minimal reconstruction error, and the highest PSNR values, reflecting superior noise suppression and better image quality across all tested images. These findings suggest that the fk4 wavelet family, when combined with the Bayes shrink method, provides a robust framework for Gaussian noise reduction in natural images. The comparative analysis highlights the importance of selecting appropriate wavelet families to optimize noise reduction performance, paving the way for further research and potential improvements in image denoising techniques.

1. Introduction

Images are invariably contaminated by noise during acquisition, compression, and transmission due to the effect of the environment, the transmission channel, and other variables. This causes distortion and loss of image information. Consequently, post-image processing tasks, including tracking, image analysis, and video processing, suffer from noise. A noisy image is unpleasant to look at, hence image de-noising is necessary [1]. Furthermore, some small details in the image might be mistaken for noise or vice versa. A clear image is necessary to function well for several image-processing techniques, including pattern recognition. Noise samples that are random and uncorrelated cannot be compressed. These issues highlight how crucial de-noising is in image and video processing. Consequently, image denoising is crucial to contemporary image processing systems [2].

The goal of image denoising is to restore the original image by eliminating noise from a noisy one. However, because texture, edge, and noise are high frequency components, it is challenging to discern them during the denoising process, and the resulting denoised images may unavoidably lose certain details. In general, one of the major issues of the modern period is recovering meaningful information from noisy photos during the noise removal process to produce high-quality photographs. Although denoising is a well-known issue that has been researched extensively, it remains a difficult and unfinished task. This is mainly because picture denoising is an inverse issue with a non-unique solution from a mathematical standpoint. The following sections provide an overview of the significant advancements made in the field of picture denoising in recent decades [3, 4]. The aims of the study are to determine which wavelet bases are appropriate and how big a neighborhood should be when using picture denoising methods to optimize PSNR and MSE.

The remainder of this paper is organized as follows. Section 2 discusses related works. In section 3, the study formulates the image denoising problem. Section 4 presents extensive experiments and discussion. Conclusions and some possible directions for future study are presented in section 5.

2. Related Works

Contrasted with image augmentation, image denoising is a subjective process, while image enhancement is an objective process [3]. An attempt is made to restore a deteriorated image through the technique of image denoising by utilizing knowledge of the degrading process that was previously acquired. The opposite of this is image augmentation, which involves changing an image's elements to improve its appeal to the human eye. The two processes do cross paths occasionally [4].

The symmetric Daubechies complex wavelet transform is used in this research to present a new approach for clearing clinical photographs in the existence of noise. The suggested technique is adaptive, using the variance of wavelet coefficients as well as the mean and median of absolute wavelet coefficients to calculate shrinkage. The proposed approach is compared to various cutting-edge deconstructing algorithms as well as the standard Wiener filter in the study. In terms of picture quality, the findings suggest that the suggested approach surpasses existing methods [5].

A multilayer soft thresholding strategy for noise reduction in Daubechies complex wavelet transform is also presented. This approach detects powerful edges by exploiting the imaginary components of complex coefficients, followed by multilayer thresholding and shrinkage on complex wavelet coefficients in the wavelet domain at non-edge positions [6].

Wavelet-based methods can be applied to various subjects. To maximize storage and transmission efficiency, large data files are typically compressed into smaller files [7]. There are several types of data compression techniques, including lossless data compression, where the original data can be precisely recreated from the compressed data when it is compressed without any loss. Because there will be data loss during lossy data compression, which compresses data before it is decompressed, the file that is recovered is not exactly the original data. Regardless of the signal's frequency components, denoising is primarily utilized to remove any existing noise and keep the important data. Bilateral filters can employ any wavelet thresholding approach as long as it is effective. Despite both bilateral and wavelet filters performing well on small noisy images, the suggested technique outperforms them on strong noisy images using the same parameters [8]. It keeps low-frequency content while having completely distinct material. Thresholding the wavelet coefficients is the most crucial step in the wavelet domain for separating information from noise. Techniques for hard and soft thresholding are primarily used.

The wavelet transform's low entropy, decoupling qualities, and multi-resolution capabilities make it a popular tool in signal analysis and image processing, by calculating the edge information, Wang, Lei. *et al.* [9] enhanced the conventional thresholding method and produced a better noise reduction result. In order to maintain the picture edges while zeroing the wavelet coefficients in non-edge regions, they enhanced the threshold. Using various families of discrete wavelet transforms, thresholding strategies, and the number of signal decomposition levels, González-Rodríguez. *et al.* [10] denoised phonocardiogram signals. They discuss how the efficiency of the denoising algorithm was affected by the wavelet function selected and the number of wavelet decomposition levels. In [11], the authors presented a new iterative approach that aggregates the smooth wavelet transform, bilateral filtering, Bayesian

estimation, and anisotropic diffusion filtering in order to reduce the scattering noise in SAR images while maintaining the image's edges and structure. Neural networks have also started to be applied to picture denoising. A method based on Deep Neural Network and wavelet transform was employed by Jin, Yanrui, *et al.* [12] to increase the accuracy of topographic image classification. [13] trained multilayer perceptron ANNs using a backpropagation technique to obtain good picture denoising without any prior knowledge of the degradation model. This illustrates how neural networks might be used in the field of denoising, which is a promising application that merits further exploration.

3. Materials and Methods

Although wavelets are helpful for signal compression, their applications are far broader. They are particularly useful in applications like medical imaging, where image degradation is not permitted. They can be used to process and improve data. They can be applied to eliminate noise from an image; for instance, wavelets can be used to successfully remove noise if the image has a very fine scale.

3.1. Wavelet Transformation (Wt)

A wavelet converter might be used as a scientific tool for analyzing progressive pictures and preparing erratic signals. Wavelets, which are tiny waves with variable recurrence and length, are what drive the change. Both the recurrence and the spatial depiction of a picture are provided by the wavelet change [14]. Time data is protected in this change, which is very different from ordinary Fourier modifications. Mother wavelets are a well-established body of work from which wavelets are constructed. This section examines the suitability of a wavelet transformation for an image watermarking and the key advantages of using a wavelet change over other modifications [15].

3.2. Single-Level 2D Discrete Wavelet Transform (2D-DWT)

The image is divided into pixels using the Discrete Wavelet Transform (DWT). DWT is employed in signal and image processing, particularly for the lossless compression of images. Lossy compression also makes use of DWT. Lossy and lossless image compression algorithms both use DWT. Images with gray levels are compressed lossless (JPEG 2000) using DWT. A discrete signal is transformed by DWT. The perfect reconstruction of the original image is made possible by the low-pass filtered signal L (low frequency). The high-pass filtered signal H is represented by H. The two photos used to illustrate the DWT process are represented by the two images in the DWT. The DWT image will next proceed to the quantization stage [16]. The procedure is repeated to achieve the optimum results. As a result, the DWT image compression produces good results.

The DWT partitions an image into three distinct regions of significance: namely one central area of focus and many sub-images or sub-ranges within the range of [1, 12]. There exist four distinct categories, namely LL, LH, HL, and HH. Figure 1 illustrates the sub-bands of the DWT. In both the horizontal and vertical dimensions, the occurrence of LL exhibits low frequency. Both the vertical and horizontal components of HH exhibit high frequencies. In terms of the horizontal axis, HL exhibits high frequencies, however, in the vertical axis, it demonstrates lower frequencies. LH exhibits low frequencies in a horizontal direction, while vertical tracks are characterized by high frequencies. The presence of undesirable data within the signal is observed within the low-frequency range. The high-frequency region is primarily composed of the edge components. The LL tape holds significant importance as it establishes a connection with the picture and encapsulates the majority of its vibrancy. Watermarks can be incorporated into the LH, HL, and HH high-frequency detail groups, as these groups exhibit reduced sensitivity to visual perception.

High-pass and low-pass filters are utilized for signal transmission. After that, the image is separated into low-frequency (approximation) and high-frequency (details) components. Each level receives four sub-signals. The approximation displays the horizontal, vertical, and diagonal component details as well as the general trend of the pixel values, this figure finds by author by using MATLAB program.

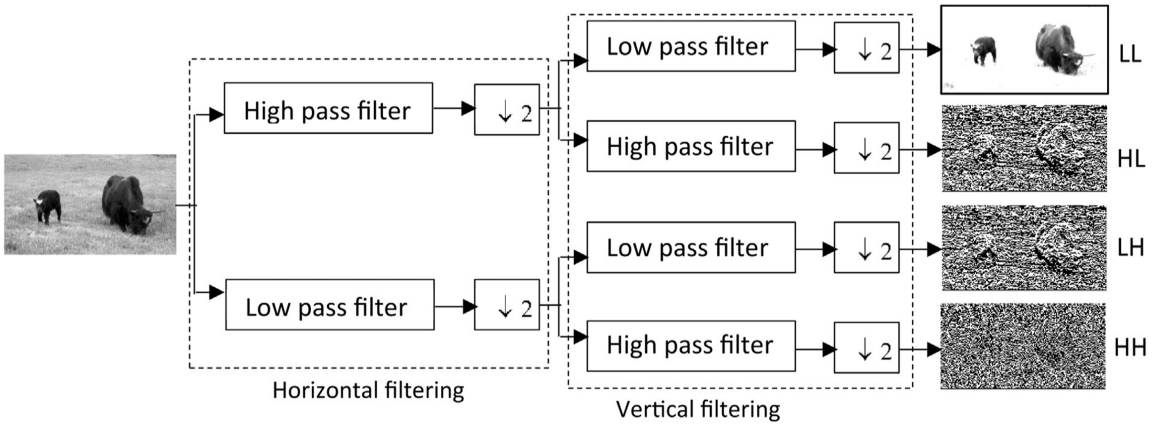

Figure 1: Decomposition of an image 2-D discrete wavelet transforms.

3.3. Selecting Wavelet Function and Number of Levels

3.3.1. Daubechies Wavelet (db)

The so-called normal orthogonal wavelets had their origins in 1988 [17], the same year that made possible the use of discrete wavelet analysis, and are named after Ingrid Daubechies, a pioneer in the study of wavelength. For instance, db4 represents the initials of the researcher (Daubechies) and the number of vanishing or ephemeral moments of the wavelet function respectively, (N) is the length of the candidate or rank, and (L_1) is the number of ephemeral moments of the wavelet function (db2). In the following relations, (L_1) corresponds to the same person as (N), who is the second-ranked person in this family [18].

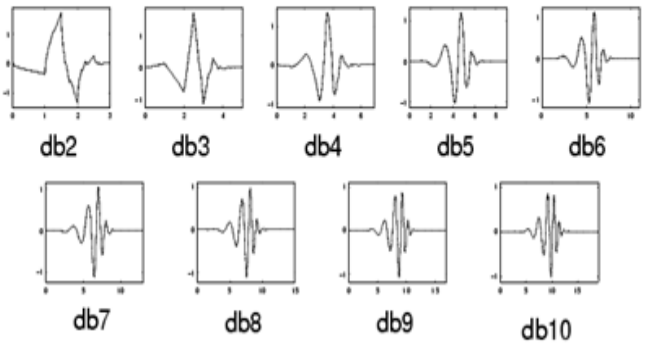

Figure 2: Daubechies wavelets family (from order 2 to 10) signal analysis using MATLAB.

3.3.2. Fejér-Korovkin Wavelet (fk)

In discrete (decimated and un-decimated) wavelet packet transforms, filters are built to minimize the difference between a valid scaling filter and the ideal since low-pass filters, and filters having N coefficients are very important. We use the well-known Fejér-Korovkin kernels from approximation theory to build a series of filters with optimal resolution. Name of the Fejér-Korovkin filter for scaling $\boldsymbol{L_0}$= Fejér-Korovkin (wavelet name). Each name includes a number that corresponds to the number of Fejér-Korovkin filter coefficients. The wavelet name specifies the Fejér-Korovkin filter to be returned. The fk4, fk6, fk8, fk14, fk18, and fk22 are all acceptable. Values for wavelet name, where N might be any of 4, 6, 8, 14, 18, or 22. Both the Fejér-Korovkin filters and the $\boldsymbol{L_0}$ 0 scaling filter are returned in a vector format [19].

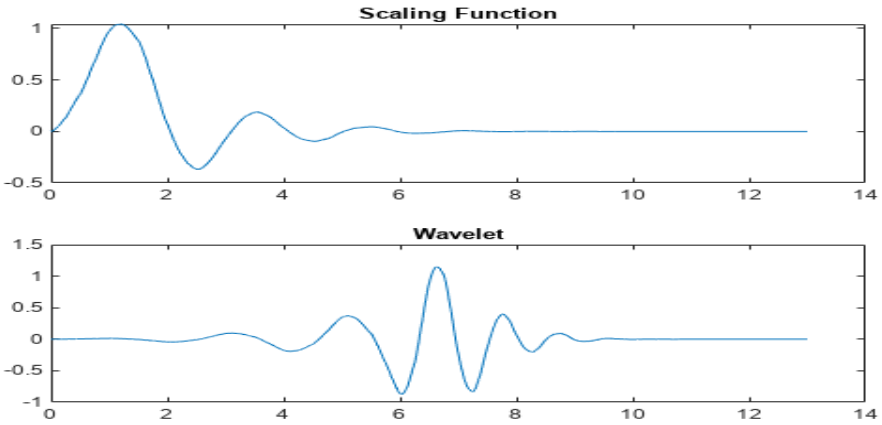

Figure 3: Fejer-Korovkin Wavelet (fk), this figure find by using MATLAB program.

3.3.3. Coiflet Wavelet

The Coiflet wavelet function possesses 2N moments with a value of 0, while the scaling function possesses 2N-1 moments with a value of 0. Additionally, both functions have a support of length 6N-1. The wavelet function exhibits the maximum number of vanishing moments for both phi and psi, within a specified support width [20].

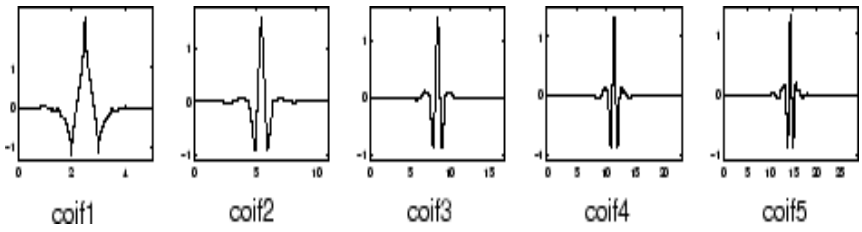

Figure 4: Coiflet Wavelet (coif), this figure finds by using MATLAB program.

3.4. Bayes Shrink Thresholding Rule

Wavelet soft-thresholding for image denoising employs the adaptive data-driven threshold known as BayesShrink. The threshold is determined using a Bayesian framework, and we aim to determine the threshold that reduces the Bayesian risk by assuming a generalized Gaussian distribution for the wavelet coefficients in each detail [21]. This is how Bayes shrink is calculated in equation (1):

$$\sigma_{noise}^2 = \sigma_{oinal}^2 + \eta \qquad [21]\ (1)$$

3.4. Image Denoising

A wide range of actions, including digitization, duplication, transmission, and viewing, are included in image handling. Tragically, this approach generally degrades image quality by masking different types of noise [22]. Unwanted noise must be identified and eliminated in this way to restore the original visual structure. Filter-based noise reduction techniques are used in image management to achieve commotion expulsion. With the help of a wavelet, a large number of small factors can be reduced to a smaller number of large ones. The wavelet transform is used in general denoising techniques, and the following steps are involved [23]. In figure. 5, we show the steps of denoting the image that we have used in this study, this figure draws by author.

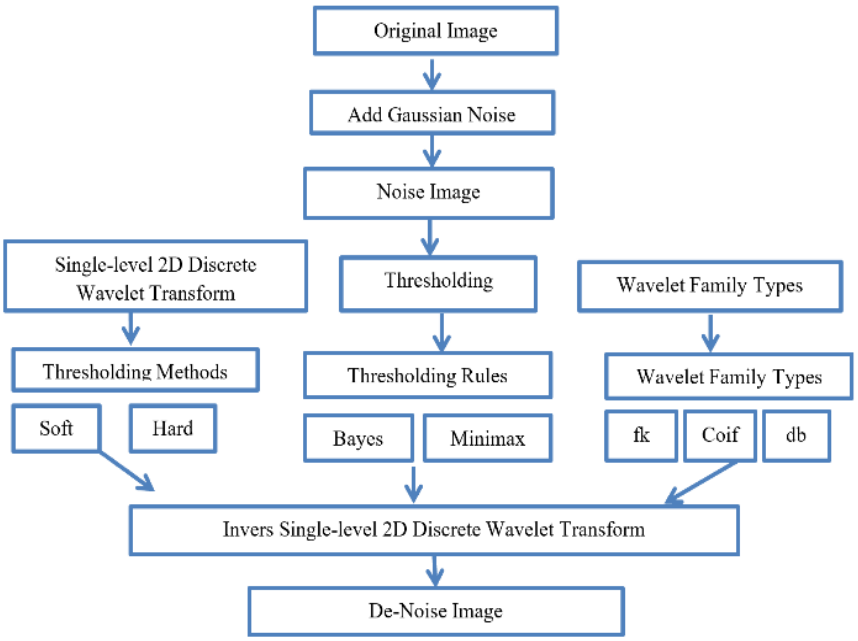

Figure 5: Block diagram of the image denoising.

3.5. Evaluation Criteria

The peak signal-to-noise ratio (PSNR) block computes the ratio between two images and represents it in decibels (dB). The aforementioned ratio is employed to compare the quality of the original image with that of its compressed counterpart. As PSNR increases, there is an observable enhancement in the image quality of the compressed or reconstructed image.

The evaluation of image compression quality commonly employs two metrics: mean-square error (MSE) and PSNR. The PSNR is a metric that quantifies the maximum error in a signal, whereas the Bit Error Rate is a metric that quantifies the average error in a signal. The MSE quantifies the overall squared discrepancy between the original image and the compressed image. The occurrence of error diminishes as the MSE decreases. The block performs the calculation of the mean-squared error before the computation of the PSNR.

$$PSNR = 10log_{10}\frac{R^2}{MSE} \quad (2)$$

In equation (2), R is the maximum fluctuation in the input image data type. For example, if the input image has a double-precision floating-point data type, then R is 1. If it has an 8-bit unsigned integer data type, R is 255, etc.

4. Results

High-resolution MRI, pediatric, and pepper test images are utilized in the experimental studies. The noise introduced to the original test images follows a Gaussian distribution. The images are transformed into two dimensions using wavelet transform. The wavelet coefficients are then adjusted with Bayes shrink threshold and both soft and hard thresholding rules, by the shrinking of neighboring coefficients. The denoised image is reconstructed using these newly adjusted coefficients. To assess the method's effectiveness, the PSNR and MSE are measured. For this purpose, MATLAB software (version 2020a) was developed specifically for this project. The threshold parameters for the evaluated methods are listed in table 1.

Table 1: Threshold parameters of evaluated methods.

Method	Value
Wavelet Transform	0.54
Gaussian Filter	0.48

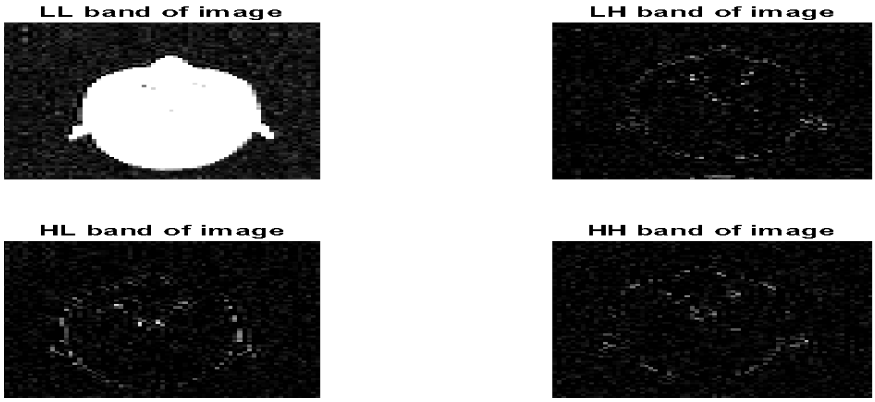

Figure 6: Four bands split of MRI Image.

As displayed MRI Image in figure 6, each column of the transformed image is horizontally transformed in the second stage of the first level of decomposition using the same horizontal filter bank. As a result, the initial decomposition step produces four filtered and subsampled images. This figure was generated by the author using the MATLAB program.

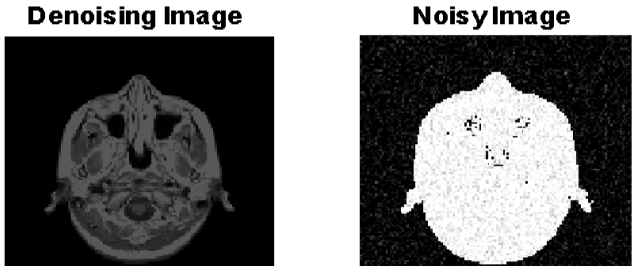

Figure 7: Result of denoising MRI Image.

Figure 7 shows the images of the original image before and after it was denoised to the best of their ability, this figure is found by the author by using the MATLAB program.

Table 2: Result analysis of image MRI compression for various wavelet transforms.

Gaussian Noise (Mean = 0, Var = 0.05)					
Name Image	**Threshold Rules**	**Threshold Method**	**Wavelet Family Name**	**MSE**	**PSNR**
MRI Image	Bayes Shrink	Soft	db7	2.0052e-25	295.1092
			fk4	8.3611e-33	368.9082
			Coif5	4.3201e-18	221.7759
		Hard	db7	1.9712e-25	295.1834
			fk4	8.3341e-33	368.9222
			Coif5	4.5625e-18	221.5387
	Minmax shrink	Soft	db7	1.9560e-25	295.2171
			fk4	8.7869e-33	368.6925
			Coif5	4.5611e-18	221.5401
		Hard	db7	1.9683e-25	295.1898
			fk4	8.5792e-33	368.7963
			Coif5	4.4356e-18	221.6613

In Table 2, the (fk4) wavelet has shown the best results in terms of PSNR and MSE values across all cases, based on the estimated image quality measurement parameters. For optimal compression, the peak signal-to-noise ratio should be as high as possible, and the mean square error should be as low as possible. These results were obtained by the author using the MATLAB program.

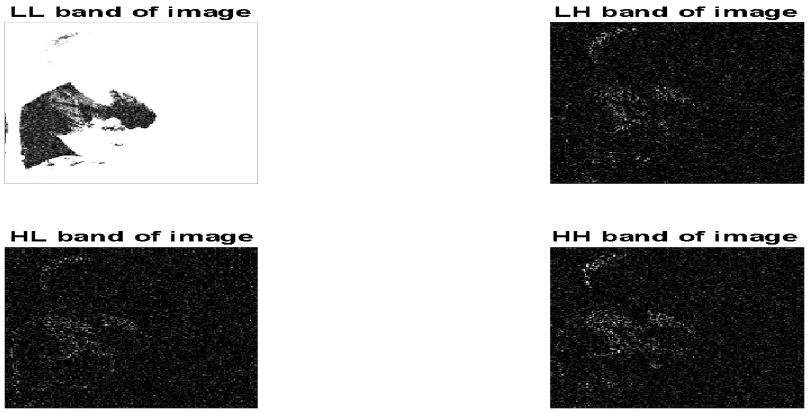

Figure 8: Four bands split of KIDS image.

The second stage of the first level of decomposition involves horizontally transforming each column of the transformed image using the same horizontal filter bank. The second action is: As a result, the first stage of decomposition yields four filtered and subsampled, this figure finds by author by using MATLAB program, the results shown in figure 8.

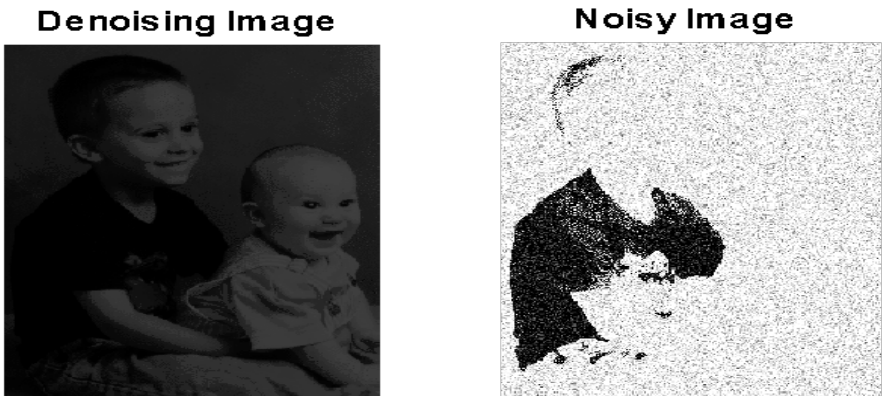

Figure 9: Result of denoising KIDS image.

Figure 9 shows the images of the original image before and after it was denoised to the best of their ability, this figure was found by the author by using the MATLAB program.

Table 3: Result analysis of image KIDS compression for various wavelet transforms.

Gaussian Noise (Mean=0, Var=0.05)					
Name Image	**Threshold Rules**	**Threshold Method**	**Wavelet Family Name**	**MSE**	**PSNR**
KIDS Image	Bayes Shrink	Soft	db7	1.9865e-25	295.1500
			fk4	1.8584e-32	365.4394
			Coif5	4.9858e-18	221.1535
		Hard	db7	1.9858e-25	295.1514
			fk4	1.8498e-32	365.4596
			Coif5	4.9098e-18	221.2202
	Minmax shrink	Soft	db7	1.9961e-25	295.1291
			fk4	1.8704e-32	365.4115
			Coif5	4.9228e-18	221.2087
		Hard	db7	1.9873e-25	295.1482
			fk4	1.8496e-32	365.4599
			Coif5	4.9773e-18	221.1608

Based on the estimated values of the picture quality measurement parameters, table 3 showed that the (fk4) wavelet had the best overall PSNR and MSE values. The author used the MATLAB tool to generate this table, which shows that the peak signal-to-noise ratio and the mean square error should be as high and low as possible, respectively, for optimal compression.

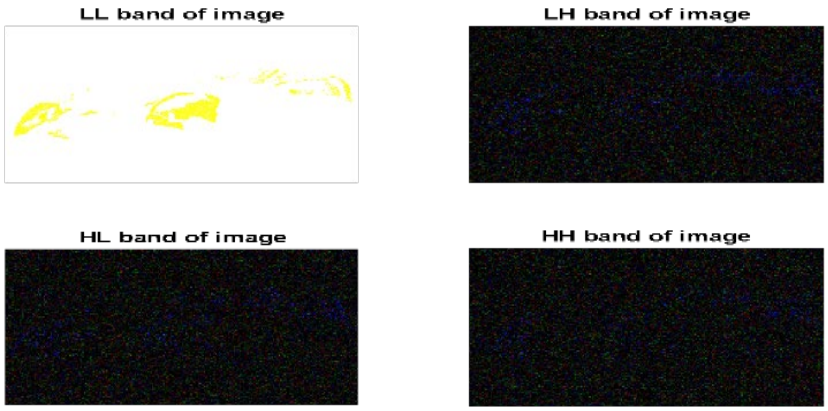

Figure10: Four bands split of PEPPERS Image.

In the second stage of the first level of decomposition, every column of the transformed image is horizontally transformed using the same horizontal filter bank. Shown is the second action in figure 10. Thus, the first level of decomposition results in the generation of four filtered and sub-sampled images, as this table shows, which the author discovered using a MATLAB program.

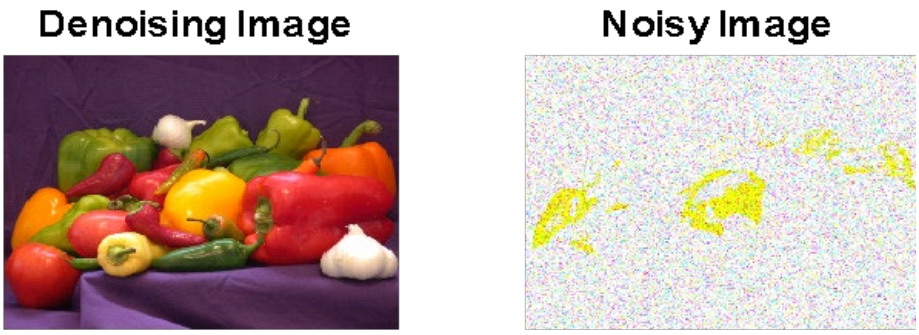

Figure 11: Result of de-noising peppers image.

Figure 11 shows the images of the original image before and after it were denoised to the best of their ability, this table finds by author by using MATLAB program.

Table 4: Result analysis of image PEPPERS compression for various wavelets transform.

Gaussian Noise (Mean = 0, Var = 0.05)					
Name Image	**Threshold Rules**	**Threshold Method**	**Wavelet Family Name**	**MSE**	**PSNR**
PEPPERS Image	Bayes Shrink	Soft	db7	1.4759e-25	296.4404
			fk4	2.1248e-32	364.8576
			Coif5	3.8174e-18	222.3132
		Hard	db7	1.4834e-25	296.4182
			fk4	2.1264e-32	364.8544
			Coif5	3.7880e-18	222.3467
	Minmax shrink	Soft	db7	1.4739e-25	296.4461
			fk4	2.1220e-32	364.8633
			Coif5	3.8188e-18	222.3116
		Hard	db7	1.4788e-25	296.4317
			fk4	2.1324e-32	364.8421
			Coif5	3.8036e-18	222.3289

In table 4, the (fk4) wavelet exhibited the best PSNR and MSE values across the board, based on the estimated values of the image quality measurement parameters. For optimal compression, the PNSR must be as high as possible, and the mean square error must be as small as possible. This table was created by the author by MATLAB.

5. Discussion

The findings of this study demonstrate the effectiveness of a single-level 2D DWT approach combined with wavelet shrinkage for denoising natural images corrupted by Gaussian noise. The comparative analysis revealed that the Fejer-Korovkin (fk4) wavelet consistently outperformed Daubechies (db7) and Coiflets (coif5) wavelets in terms of PSNR and MSE metrics across all test images (MRI, pediatric, and peppers). This suggests that the fk4 wavelet family possesses superior characteristics for capturing and removing noise in the wavelet domain, leading to improved image fidelity after reconstruction.

These results highlight the crucial role of wavelet family selection in optimizing image denoising performance. Future research directions could explore the application of more sophisticated thresholding techniques, such as Vis Shrink or Sure Shrink, in conjunction with the fk4 wavelet for potentially even

greater noise reduction capabilities. Additionally, investigating the performance of this approach with different noise distributions and image types could provide valuable insights into its broader applicability in image processing tasks.

6. Conclusions

In this paper, a single-level 2D discrete wavelet transform (DWT) was presented for the removal of image noise from a variety of images. The transform employed three wavelet types (db7, coif5, and fk4) as well as Bayes and Minimax shrinkage thresholding methods with soft and hard thresholding rules. The use of the fk4 wavelet demonstrated superior capability in retaining image details while effectively reducing noise, likely due to its specific characteristics that align well with the frequency components typical in common image noise. This finding is significant as it highlights the importance of selecting appropriate wavelet types for different noise patterns and image characteristics. Furthermore, the superiority of Bayes thresholding with a hard thresholding rule underscores the necessity of adaptive thresholding strategies tailored to the statistical properties of the noise. The hard thresholding rule, while simple, appears to balance noise reduction and detail preservation efficiently under the Bayes shrinkage method, suggesting its potential for broader applications in practical image denoising tasks. The implementation of the single-level 2D discrete wavelet transform demonstrates significant potential for enhancing image quality by effectively reducing noise while preserving critical image details. The choice of fk4 wavelet and Bayes thresholding with a hard thresholding rule highlights the importance of selecting appropriate wavelet functions and thresholding techniques tailored to the specific noise characteristics of the image. The evaluation results shows that the fk4 wavelet yields the best results in terms of PSNR and MSE values. It has also been shown that Bayes thresholding with a hard thresholding rule performs better than other methods.

Future work could explore multi-level DWT and other advanced wavelet families to potentially enhance denoising performance further. Additionally, integrating machine learning techniques to adaptively select wavelet types and thresholding methods based on image content and noise characteristics could provide a more automated and robust approach to image denoising. This study lays a solid foundation for such explorations and contributes to the ongoing efforts to improve image quality in various digital imaging applications.

Authors contributions: Hawkar Qsim Birdawod: Writing – original draft. **Azhin Mohammed Khudhur**: formal analysis. **Dler Hussein Kadir:** Supervision, formal analysis, validation. **Dlshad Mahmood Saleh:** Writing – original draft.

Data availability: The data has been used is confidential.

Conflicts of interest: The authors declare that they have no known competing financial interests or personal relationships that could have appeared to influence the work reported in this paper.

Funding: The authors did not receive support from any organization for the submitted work.

References

[1] X. Jianhui and T. Li, "Image Denoising Method Based on Improved Wavelet Threshold Transform," in *2019 IEEE Symposium Series on Computational Intelligence (SSCI)*, pp. 1064-1067, 2019, doi: 10.1109/SSCI44817.2019.9002923.

[2] A. Vyas and J. Paik, "Review of The Application of Wavelet Theory to Image Processing," *IEIE Transactions on Smart Processing and Computing*, vol. 5, no. 6, pp. 403-417, 2016, doi: 10.5573/ieiespc.2016.5.6.403.

[3] R. E. Woods and R. C. Gonzalez, *Digital Image Processing*, Pearson Education Ltd., 2008.

[4] T. Zhao, Y. Wang, Y. Ren, and Y. Liao, "Approach of Image Denoising Based on Discrete Multi-Wavelet Transform," in *2009 International Workshop on Intelligent Systems and Applications*, pp. 1-4, 2009, doi: 10.1109/IWISA.2009.5072757.

[5] A. Khare, M. Khare, Y. Jeong, H. Kim, and M. Jeon, "Despeckling of Medical Ultrasound Images Using Daubechies Complex Wavelet Transform," *Signal Processing*, vol. 90, no. 2, pp. 428-439, 2010, doi: 10.1016/j.sigpro.2009.07.008.

[6] A. Khare, U. Tiwary, W. Pedrycz, and M. Jeon, "Multilevel Adaptive Thresholding and Shrinkage Technique for Denoising Using Daubechies Complex Wavelet Transform," *Imaging Sci. J.*, vol. 58, no. 6, pp. 340-358, 2010, doi: 10.1179/136821910X12750339175826.

[7] D. L. Donoho and I. M. Johnstone, "Ideal Spatial Adaptation by Wavelet Shrinkage," *Biometrika*, vol. 81, no. 3, pp. 425-455, 1994, doi: 10.1093/biomet/81.3.425.

[8] W. T. Kahwachi and H. Q. Birdawod, "A New Hybridization of Bilateral and Wavelet Filters for Noisy De-Noisy Images," *Eurasian J. Sci. Eng.*, vol. 9, no. 1, 2023, doi: 10.23918/EAJSE.V9I1P99.

[9] L. Wang, H. Xu, and Y. Liu, "A Novel Dynamic Load Identification Approach for Multi-Source Uncertain Structures Based on The Set-Theoretical Wavelet Transform and Layered Noise Reduction," *Structures*, vol. 51, 2023, doi: 10.1016/j.istruc.2023.03.037.

[10] C. González-Rodríguez, M. A. Alonso-Arévalo, and E. García-Canseco, "Robust Denoising of Phonocardiogram Signals Using Time-Frequency Analysis and U-Nets," *IEEE Access*, vol. 11, pp. 52466-52479, 2023, doi: 10.1109/ACCESS.2023.3280453.

[11] S. L. Shabana Sulthana and M. Sucharitha, "Two-Phase Speckle Noise Removal in US Images: Speckle Reducing Improved Anisotropic Diffusion and Optimal Bayes Threshold," *Int. J. Image Graph.*, 2550071, 2024, doi: 10.1142/S0219467825500718.

[12] Y. Jin, X. Zhang, M. Liu, L. Wang, and J. Li, "A Novel Deep Wavelet Convolutional Neural Network for Actual ECG Signal Denoising," *Biomed. Signal Process. Control*, vol. 87, 105480, 2024, doi: 10.1016/j.bspc.2023.105480.

[13] S. Abut, H. Okut, and K. J. Kallail, "Paradigm Shift from Artificial Neural Networks (Anns) to Deep Convolutional Neural Networks (Dcnns) in The Field of Medical Image Processing," *Expert Systems with Applications*, 122983, 2023, doi: 10.1016/j.eswa.2023.122983.

[14] T. H. Ali, S. H. Mahmood, and A. S. Wahdi, "Using A Proposed Hybrid Method of Neural and Wavelet Networks to Estimate the Time Series Model," *Tikrit J. Admin. Econ. Sci.*, vol. 18, no. 57, 3, pp. 432-448, 2022, doi: 10.25130/tjaes.18.57.3.26.

[15] T. H. Ali and D. M. Saleh, "Comparison Between Wavelet Bayesian and Bayesian Estimators to Remedy Contamination in Linear Regression Model," *PalArch's Journal Archaeology of Egypt/Egyptology*, vol. 18, no. 10, pp. 3388-3409, 2021.

[16] M. Chowdhury, M. Hoque, and A. Khatun, "Image Compression Using Discrete Wavelet Transform," *IJCSI International Journal of Computer Science Issues*, vol. 9, pp. 327-330, 2012.

[17] I. Daubechies, "Orthonormal Bases of Compactly Supported Wavelets," *Communications on Pure and Applied Mathematics*, vol. 41, no. 7, pp. 909-996, 1988, doi: 10.1002/cpa.3160410705.

[18] T. H. Ali and D. M. Saleh, "Proposed Hybrid Method for Wavelet Shrinkage with Robust Multiple Linear Regression Model: With Simulation Study," *Qalaai Zanist Journal*, vol. 7, no. 1, pp. 920-937, 2022, doi: 10.25212/lfu.qzj.7.1.36.

[19] M. Nielsen, "On the Construction and Frequency Localization of Finite Orthogonal Quadrature Filters," *J. Approx. Theory*, vol. 108, no. 1, pp. 36-52, 2001, doi: 10.1006/jath.2000.3514.

[20] B. Anjali and S. Jagroop, "Coiflet Wavelet Transform Image Compression Based on JPEG Images," *International Journal of Advanced Research in Electrical, Electronics and Instrumentation Engineering*, vol. 5, no. 7, pp. 6358-6363, 2016, doi :10.15662/IJAREEIE.2016.0507088.

[21] A. Dixit and P. Sharma, "A Comparative Study of Wavelet Thresholding for Image Denoising," *IJ Image, Graphics and Signal Processing*, vol. 12, pp. 39-46, 2014, doi: 10.5815/ijigsp.2014.12.06.

[22] S. K. Mohideen, S. A. Perumal, and M. M. Sathik, "Image De-Noising Using Discrete Wavelet Transform," *International Journal of Computer Science and Network Security*, vol. 8, no. 1, pp. 213-216, 2008.

[23] S. D. Ruikar and D. D. Doye, "Wavelet Based Image Denoising Technique," *International Journal of Advanced Computer Science and Applications*, vol. 2, no. 3, 2011, doi: 10.14569/IJACSA.2011.020309.